The Ashkin–Teller neural network near saturation

D Bollé†§ and P Kozłowski†‡§

† Instituut voor Theoretische Fysica, K U Leuven, B-3001 Leuven, Belgium
‡ Computational Physics Division, Institute of Physics, A Mickiewicz University, PL 61-624
Poznań, Poland

E-mail: `desire.bolle@fys.kuleuven.ac.be` and
`piotr.kozlowski@fys.kuleuven.ac.be`

Abstract. The thermodynamic and retrieval properties of the Ashkin–Teller neural network model storing an infinite number of patterns are examined in the replica-symmetric mean-field approximation. In particular, for linked patterns temperature-capacity phase diagrams are derived for different values of the two-neuron and four-neuron coupling strengths. This model can be considered as a particular non-trivial generalization of the Hopfield model and exhibits a number of interesting new features. Some aspects of replica-symmetry breaking are discussed.

1. Introduction

The Ashkin–Teller neural network (ATNN) studied recently by us in the case of loading of a finite number of patterns ([1] and references therein) can be considered as a non-trivial generalization of the Hopfield model [2, 3] to allow for different types of neurons. It can be seen as a model consisting of two Hopfield models interacting through a four-neuron term, or it can be interpreted as a neural network with two types of neurons at each site having different functions.

Some of the underlying neurobiological motivation for the introduction of different types of neurons is the fact that there exist areas in the brain which react to two different kinds of dependent stimuli in such a way that the response to particular combinations of these stimuli is stronger than the response to others [4]. Furthermore, in neuropsychological studies on amnesia it has become appreciated that memory is composed of multiple separate systems which can store different types of information: e.g., information based on skills and information based on specific facts or data [5]. In addition, the classical Ashkin–Teller model, on which our ATNN model is based, appears in studies of disordered systems when the disorder evolves on a time scale that can be tuned [6]. Finally, two different types of neurons show up naturally when considering the Hopfield model with synchronous dynamics [3, 7, 8].

Storage and retrieval of embedded patterns built from these two types of neurons with different degrees of (in)dependence have been discussed in [1] for finite loading: i.e. the capacity α, defined as the number of embedded patterns, p, versus the size of the system, N, is taken to be zero. In that study we wanted to find out, e.g., whether the four-neuron interaction between the two types of neuron can improve the retrieval process. And indeed, it has been seen that interesting retrieval behaviour emerges, especially for linked patterns: e.g., different

§ Also at Interdisciplinair Centrum voor Neurale Netwerken, K U Leuven, Belgium.

types of Mattis states occur, a higher retrieval transition temperature is possible, the quality of retrieval is improved through a bigger overlap. Therefore, it is interesting to investigate the properties of this model for infinite loading of patterns, i.e., for $\alpha \neq 0$. This is the purpose of the present paper.

After describing the ATNN model in section 2 we use the standard replica mean-field theory approach in order to write down its free energy in section 3. Assuming replica symmetry we then obtain the fixed-point equations for the relevant order parameters. Thermodynamic and retrieval properties are discussed in section 4. In particular, section 4.1 investigates the behaviour of the model at zero temperature for equal two- and four-neuron coupling strengths in the Hamiltonian. In this case also the entropy is calculated and found to be negative. This leads to a discussion about the size of the replica-symmetry breaking and re-entrance behaviour. Section 4.2 presents phase diagrams in the temperature–capacity plane for different values of the two-and four-neuron coupling strengths. A number of new features in these diagrams show up. Also, the maximal information content of the network is obtained as a function of these couplings. Where relevant, the results are compared with the Hopfield model [2, 3] and with the four-state Potts model [9–11]. Finally, section 5 presents some concluding remarks.

2. The model

We consider a network of N sites each with two different types of binary neurons s_i and σ_i, $i = 1, \ldots, N$. The interactions between the neurons are determined by the infinite-range Hamiltonian

$$H = -\tfrac{1}{2} \sum_{i \neq j} [J_{ij}^{(1)} s_i s_j + J_{ij}^{(2)} \sigma_i \sigma_j + J_{ij}^{(3)} s_i s_j \sigma_i \sigma_j]. \tag{1}$$

In this network storage and retrieval of two different types of patterns, $\boldsymbol{\xi}_i = \{\xi_i^\mu\}$ and $\boldsymbol{\eta}_i = \{\eta_i^\mu\}$, $\mu = 1, \ldots, p$ are enabled by a Hebb-like learning rule for the couplings

$$J_{ij}^{(1)} = \frac{1}{N} J_1 \sum_{\mu=1}^{p} \xi_i^\mu \xi_j^\mu \qquad J_{ij}^{(2)} = \frac{1}{N} J_2 \sum_{\mu=1}^{p} \eta_i^\mu \eta_j^\mu \qquad J_{ij}^{(3)} = \frac{1}{N} J_3 \sum_{\mu=1}^{p} \xi_i^\mu \eta_i^\mu \xi_j^\mu \eta_j^\mu. \tag{2}$$

The patterns $\boldsymbol{\xi}_i$ and $\boldsymbol{\eta}_i$ are supposed to be independent identically distributed random variables taking the values $+1$ or -1 with equal probability. All J_ν, $\nu = 1, 2, 3$ are non-negative.

First, we remark that the above definition of $J_{ij}^{(3)}$ is equivalent to the case of linked patterns considered in [1]. Second, we repeat that this model can be considered as an assembly of two Hopfield models (when $J_3 = 0$) interconnected via a four-neuron interaction (when $J_3 \neq 0$).

3. Replica-symmetric mean-field theory

In order to determine the thermodynamic and retrieval properties of the model we calculate the quenched free energy per site within the replica-symmetric mean-field theory approach. Using standard techniques [3] we arrive at

$$\beta f(\beta) = \frac{1}{2} \sum_{\nu=1}^{3} \left\{ \sum_{\mu=1}^{c} K_\nu (m_\nu^\mu)^2 + \frac{3}{2} \alpha \left[K_\nu + K_\nu^2 r_\nu (1 - q_\nu) - \frac{K_\nu q_\nu}{1 - K_\nu (1 - q_\nu)} \right. \right.$$

$$\left. \left. + \ln[1 - K_\nu (1 - q_\nu)] \right] \right\} - \int \prod_{\gamma=1}^{3} \mathrm{D}z_\gamma \left\langle\!\left\langle \ln \left[4 \prod_{\nu=1}^{3} \cosh a_\nu \left(1 + \prod_{\nu=1}^{3} \tanh a_\nu \right) \right] \right\rangle\!\right\rangle$$

$$\tag{3}$$

with $\beta = 1/T$ the inverse temperature measuring the noise level in the system, α the capacity defined as the number of patterns per number of couplings per spin, i.e. $\alpha = 2p/3N$ and where

$$a_\nu = K_\nu \left(\sum_{\mu=1}^c m_\nu^\mu \psi_\nu^\mu + z_\nu \sqrt{\frac{3}{2}\alpha r_\nu} \right) \tag{4}$$

$$K_\nu = \beta J_\nu \qquad \psi_1^\mu = \xi^\mu \qquad \psi_2^\mu = \eta^\mu \qquad \psi_3^\mu = \xi^\mu \eta^\mu. \tag{5}$$

Here the index $\mu = 1, \ldots, c$, c finite, labels the condensed patterns, the index $\nu = 1, 2, 3$, $\langle\langle \cdots \rangle\rangle$ indicates the average over the embedded patterns and $\mathrm{D}z_\gamma$ denotes the Gaussian measure $\mathrm{D}z_\gamma = \mathrm{d}z_\gamma (2\pi)^{-1/2} \exp(-z_\gamma^2/2)$. In (3), (4) the $\boldsymbol{m}_\nu = \{m_\nu^\mu\}$ are the overlap order parameters between the pattern ψ_ν and the network state $\{S_i^\nu\}$, the q_ν represent the Edwards–Anderson (EA) order parameters with their conjugate variables r_ν (the mean-square random overlap with the non-condensed patterns), namely

$$\boldsymbol{m}_\nu = \left\langle\!\!\left\langle \frac{1}{N} \sum_{i=1}^N \langle S_i^\nu \rangle \psi_i \right\rangle\!\!\right\rangle \qquad q_\nu = \left\langle\!\!\left\langle \frac{1}{N} \sum_{i=1}^N (\langle S_i^\nu \rangle)^2 \right\rangle\!\!\right\rangle \qquad r_\nu = \frac{2}{3\alpha} \sum_{\mu=c+1}^p \langle\langle (m_\nu^\mu)^2 \rangle\rangle \tag{6}$$

with $S_i^1 = s_i$, $S_i^2 = \sigma_i$, $S_i^3 = s_i\sigma_i$ and where $\langle \cdots \rangle$ denotes the thermal average.

The phase structure of the network is determined by that solution of the set of fixed-point equations

$$\boldsymbol{m}_\nu = \int \prod_{\gamma=1}^3 \mathrm{D}z_\gamma \left\langle\!\!\left\langle \psi_\nu \frac{\tanh a_\nu + \tanh a_\delta \tanh a_\rho}{1 + \tanh a_\nu \tanh a_\delta \tanh a_\rho} \right\rangle\!\!\right\rangle \tag{7}$$

$$q_\nu = \int \prod_{\gamma=1}^3 \mathrm{D}z_\gamma \left\langle\!\!\left\langle \left(\frac{\tanh a_\nu + \tanh a_\delta \tanh a_\rho}{1 + \tanh a_\nu \tanh a_\delta \tanh a_\rho} \right)^2 \right\rangle\!\!\right\rangle \tag{8}$$

$$r_\nu = q_\nu [1 - K_\nu(1 - q_\nu)]^{-2} \tag{9}$$

which maximizes $-\beta f(\beta)$. Here $\nu, \delta, \rho = 1, 2, 3$ and our convention is that they have to be taken different in the equations above.

Solving this set of equations is a tedious task. In the following sections we discuss these solutions that are important for the thermodynamic and retrieval properties of the model: i.e., Mattis retrieval states and spin glass (SG) states. At this point we remark that in the $\alpha = 0$ limit the replica-symmetric solution of the ATNN model presented above is completely consistent with the corresponding result obtained in [1].

4. Results

The solution of the fixed-point equations for the ATNN neural network model presented in the previous section depends, of course, on the values of the coupling strengths K_ν. Without loss of generality we put $K_1 = K_2$ in what follows. Such a choice is very often used in the literature concerning classical ([12] and references therein) and SG [13] Ashkin–Teller models. This model contains as particular limits the Hopfield network for any two K_ν equal to zero, the four-state clock network [14] (or, equivalently, two independent Hopfield networks) for any $K_\nu = 0$ and a model strongly resembling the four-state Potts network [9, 10] for $K_1 = K_2 = K_3$. We remark, however, that only the strength of the couplings is the same but, in general, $J_{ij}^{(1)} \neq J_{ij}^{(2)} \neq J_{ij}^{(3)}$ (cf [13]). Therefore, some details of the phase diagram compared with those of the Potts network may be different.

The type of solutions we are interested in, at first instance, are Mattis solutions, for which not more than one component of each order parameter m_ν is non-zero. As in [1] we thereby distinguish two types of Mattis states. Simple Mattis states where only the same components of the m_ν are non-zero, e.g., $m_1 = (m_1, 0, \ldots, 0)$, $m_2 = (m_2, 0, \ldots, 0)$, $m_3 = (m_3, 0, \ldots, 0)$, and crossed Mattis states where the same components of the m_ν are never non-zero: e.g., $m_1 = (m_1, 0, \ldots, 0)$, $m_2 = (0, m_2, 0, \ldots, 0)$, $m_3 = (0, 0, m_3, 0, \ldots, 0)$. These states are denoted by $m_1 m_2 m_3$ in what follows. All these Mattis retrieval solutions also have non-zero values of the EA order parameters q_ν. We remark that we have also found Mattis states where only one m_ν and the corresponding q_ν are non-zero. These are, in fact, Hopfield-like solutions. Furthermore, we are interested in SG states characterized by $m_\nu = 0$, $q_\nu \neq 0$ (here also Hopfield-like SG states are possible) and a paramagnetic state with all order parameters $m_\nu = 0$, $q_\nu = 0$.

First, it is worthwhile to discuss the most simple case: i.e., zero temperature with equal coupling strengths. Second, we present results for non-zero temperatures and arbitrary couplings.

4.1. Retrieval properties at zero temperature

Restricting ourselves first to $K_1 = K_2 = K_3$ we find that only solutions with equal order parameters, $m_1 = m_2 = m_3$ and $q_1 = q_2 = q_3$ exist. Further, considering simple Mattis states at zero temperature the set of fixed-point equations (7)–(9) can be reduced to a single equation, as in [3]

$$
x\sqrt{3\alpha} = \int_{-\infty}^{\infty} Dz\, \mathrm{erf}\left(\frac{z}{\sqrt{2}} + 2x\right) - \int_{-x\sqrt{2}}^{\infty} Dz\, \mathrm{erf}\left(\frac{z}{\sqrt{2}} + 2x\right)[1 - zx\sqrt{2}] + \frac{1}{2}
$$
$$
\times \int_{-\infty}^{-x\sqrt{2}} Dz\left[\mathrm{erf}^2\left(\frac{z}{\sqrt{2}} + 2x\right) + \mathrm{erf}^2\left(\frac{z}{\sqrt{2}}\right)\right][1 - zx\sqrt{2}] - x\sqrt{\frac{2}{\pi}}(1 + e^{-2x^2})
$$

$$(10)$$

with the new variable $x = m/\sqrt{3\alpha r}$ being different from zero only when $m \neq 0$. Thus the range in x allowing the existence of non-zero solutions of equation (10) determines the critical capacity, $\alpha_c(0)$, of the ATNN model with equal coupling strengths at $T = 0$. Numerically solving this equation for different values of α we find $\alpha_c(0) = 0.183\,9205$. This is higher than the critical capacity of the Hopfield model ($\alpha_c(0) = 0.137\,905\,566$) [15, 16] and agrees (up to numerical precision) with the result obtained in [9] for the four-state Potts neural network after an appropriate rescaling with the number of couplings as discussed in [17]. (The relation between the Hopfield and Potts critical capacities is given in equation (19) of [9].) We remark that taking the coupling strengths K_ν unequal always leads to a smaller critical capacity, as we will see in the next section.

In analogy with the Ashkin–Teller SG [13] and with the Hopfield network [3] we expect replica symmetry to be broken for low temperatures. Consequently, we expect some re-entrant SG behaviour (see, e.g., [18]) indicating that the true critical capacity is greater than its replica-symmetric value at $T = 0$. In order to get an idea about this breaking we have calculated the entropy of the replica-symmetric solution at $T = 0$, which for simple Mattis states reads

$$
S(\alpha) = -\frac{9}{4}\alpha\left[\ln(1 - C) + \frac{C}{1 - C}\right] \qquad C = \lim_{\beta \to \infty} \beta(1 - q). \tag{11}
$$

As expected, we find that the value of this entropy is negative. In particular, $S(\alpha_c(0)) = -0.007\,228$ versus $-0.001\,445$ for the Hopfield model [3], $-0.003\,995$ for the three-state Potts model [10] and $-0.007\,212$ for the four-state Potts model [11]. Furthermore, this
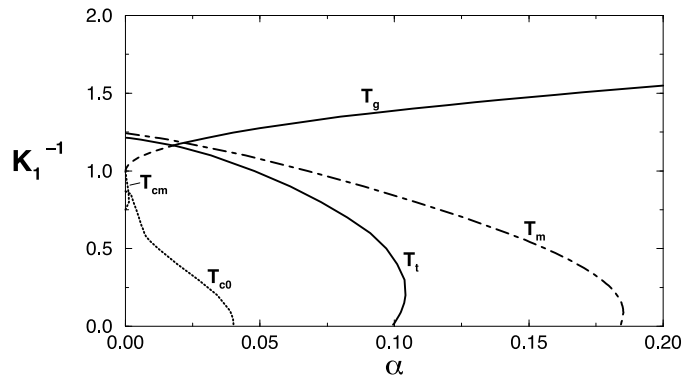
Figure 1. The T–α section of the phase diagram for the ATNN model with equal coupling strengths ($w = 1$). The solid curves indicate the thermodynamic transitions. The precise meaning of the curves is described in the text.

entropy vanishes exponentially with decreasing α and, in fact, for small α we have that $S \approx -\exp(-1/\alpha)$. In the SG phase, $S = -0.91$ at $\alpha_c(0)$ versus -0.07 for the Hopfield model [3] and -0.13 [10] for the three-state Potts model. All this suggests that replica-symmetry breaking of the retrieval states of the ATNN model is somewhat stronger than in the Hopfield model but still weak compared with the SG state of the ATNN. Further details on this matter are beyond the scope of this paper.

4.2. The phase diagram for non-zero temperatures

The phase diagram of the ATNN model is obtained by numerically solving the set of fixed-point equations (7)–(9). It is a complicated function of $K_1 = K_2$, K_3, and α, the behaviour of which we analyse by looking specifically at T–α sections for different values of the ratio $w = K_1/K_3$. Furthermore, we discuss the maximal information content of the network in the full space of couplings.

An extensive numerical analysis allows us to distinguish essentially two qualitatively different T–α sections of the full phase diagram. They are shown in figures 1 and 4.

Several transition curves bordering different phases show up. The curves T_m and T_t are related to simple Mattis solutions, the curve T_g separates the SG and paramagnetic solutions. The curves T_{c0} and T_{cm} are connected with crossed states. Finally, the curves T_{m1}, T_{g1} and T_{t1} relate to the Hopfield-like retrieval and SG solutions introduced before. We remark that, from now on, writing that a solution exists also implies that it is stable within the replica-symmetric approximation, unless stated otherwise.

Let us first discuss figure 1 where the coupling strengths are all equal, and hence $w = 1$, in more detail. We start by looking at high T expressed in units of $K_1^{-1} = T/J_1$. The transition from the disordered paramagnetic phase to the SG phase ($m_v = 0$, $q_v \neq 0$) is continuous and denoted by T_g. When crossing the curve T_m simple Mattis retrieval states show up as local minima of the free energy. At these points the overlap with the embedded patterns jumps from zero to a finite macroscopic value. So the system functions as an associative memory and the critical storage capacity for a given temperature can be read off through that line.

When further lowering T the simple Mattis states become global minima of the free energy. This happens along the curve T_t and this thermodynamic transition is first order. Here we note that the critical curves T_t and T_g end in different temperature points at $\alpha = 0$ giving rise to a 'crossover' region for small α as it occurs in the Potts model [10]. This is related to the fact
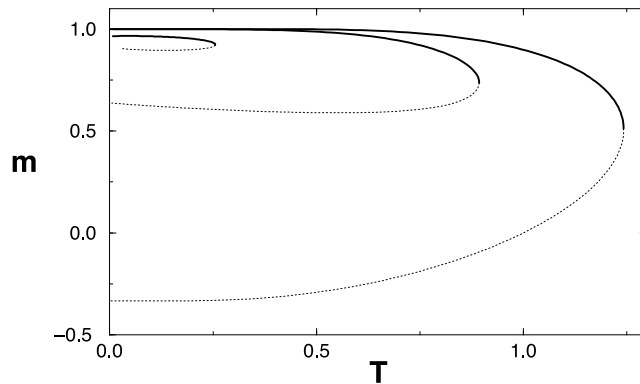
Figure 2. Typical overlap profiles as a function of the temperature for simple Mattis states of the model with $w = 1$ for different capacities. From bottom to top: $\alpha = 0, 0.09, 0.18$. The dotted parts of the curves are unstable within replica symmetry.

that for $\alpha = 0$ this ATNN model with $w = 1$ has a discontinuous transition at T_t as shown in [1] (see, in particular, figure 5). In this crossover region the simple Mattis states (global minima) and the paramagnetic state (local minimum) coexist.

Finally, at still lower T (and appropriate values of α) crossed states of the type *mmm* and *mm*0 exist left from the curves T_{cm} and T_{c0}, respectively. Their free energy is bigger than that of the simple Mattis states.

We end the discussion of this phase diagram by remarking that we find weak re-entrant behaviour both at the curves T_t and T_m. The re-entrance at the curve T_t is somewhat stronger and may suggest [19] a greater replica-symmetry breaking of the SG solution, in agreement with the values of the zero-temperature entropy calculated in section 4.1. Furthermore, the greatest capacity of the ATNN model with equal coupling strengths is obtained for temperature $T = 0.09$ and reads $\alpha_c(T = 0.09) = 0.1851$.

In figures 2 and 3 we present some typical overlap profiles for simple and crossed Mattis states in this model indicating the stability of the solutions within the replica-symmetric approximation (i.e., indicating where the solution is a minimum of the replica-symmetric free energy). We see that, for the same values of T and α, the simple states always have the largest overlap.

Next, we turn to a discussion of the phase diagram for the ATNN model with unequal coupling strengths. We explicitly consider the situation of figure 4 where $w = \frac{1}{4}$ (meaning that the four-neuron term has four times the strength of the two-neuron one). Starting from high T we first meet the (new) curve T_{g1} marking the continuous transition from the disordered paramagnetic phase to a SG1 phase where only one of the q_ν is non-zero, i.e. the Hopfield-like SG-state, $m_\nu = 0$, $q_1 = q_2 = 0$, $q_3 \neq 0$. When lowering T and taking α sufficiently small, the (new) curve T_{m1} appears below which solutions with only one m_ν and corresponding q_ν different from zero: i.e., Hopfield-like Mattis states exist as local minima of the free energy. Below the thermodynamic first-order transition curve T_{t1} they become global minima of the free energy. These Hopfield phases exist in the interval $w = [0, 0.69]$. The rest of the curves which are present are similar to the ones of figure 1, whereby we remark that the simple Mattis states are now of the form *mml*. However, crossing the curve T_m from within the Hopfield-like retrieval phase we observe that the overlap $m_1 = m_2$ continuously increases from zero. Outside this region $m_1 = m_2$ immediately jumps from zero to a finite macroscopic value as is the case in figure 1. Furthermore, crossed Mattis states of the type *mml* have become unstable
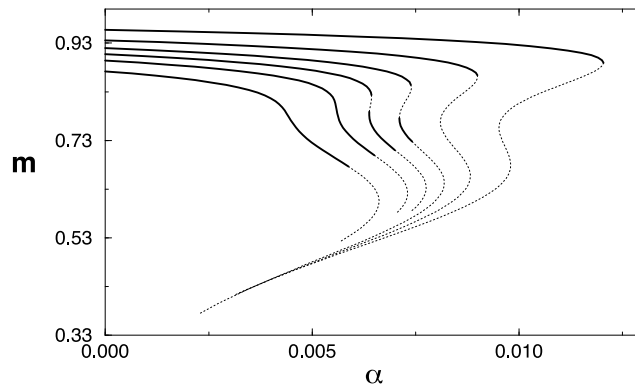
Figure 3. Typical overlap profiles as a function of the capacity for crossed Mattis states $mm0$ of the model with $w = 1$ for different temperatures. From top to bottom: $T = 0.5, 0.55, 0.58, 0.6, 0.62, 0.65$. The dotted parts of the curves are unstable within replica symmetry.
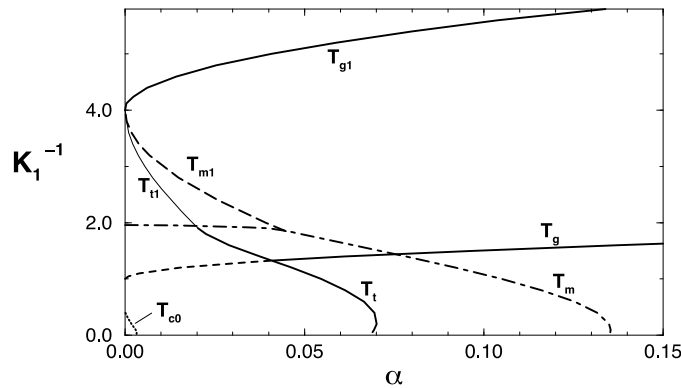

Figure 4. The T–α section of the phase diagram for the ATNN model with unequal coupling strengths ($w = \frac{1}{4}$). The solid curves indicate the thermodynamic transitions. The precise meaning of the curves is described in the text.

for this value of w whereas the crossed states of type $mm0$ exist for all $w > 0$.

Sections of the full phase diagram for different values of the ratio w are qualitatively not much different and can be explained by taking the diagram in figure 1 with $w = 1$ as a reference.

When w is increasing (starting at the value 1), meaning that the coupling strength of the four-neuron interaction becomes smaller, the crossover region shrinks since the endpoints of the curves T_g and T_m come closer. It finally shrinks to zero for $w = \infty$ meaning that one is left with two independent Hopfield models. The region where the crossed solutions $mm0$ are found gets larger such that the curve T_{c0} moves to the right until it finally coincides with the curve T_m. The shapes of the transition curves are deforming continuously in such a way that they resemble more and more the Hopfield model transition curves and finally they become identical with the latter.

When decreasing w from the value 1 the phase diagram shown in figure 1 evolves to the one presented in figure 4. The gap between the curves T_m and T_g for $\alpha = 0$ is increasing and Hopfield-like phases appear. When further decreasing w, the gap still grows until it reaches the maximal value 1 in units of K_1^{-1} and the Hopfield phase occupies a larger part of the phase
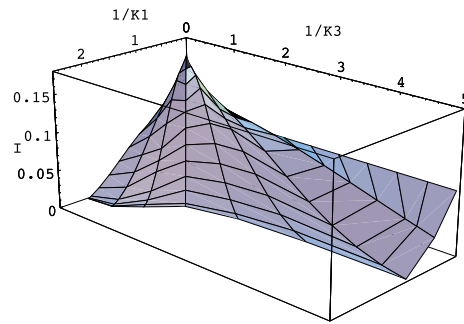
Figure 5. The maximal information content of the ATNN model as a function of K_1^{-1} and K_3^{-1}.

diagram to become completely dominating in the limit $w = 0$ where the pure Hopfield model is found. This means that the curves T_g, T_m and T_t shrink and disappear as $w \to 0$ and as a result the curves T_{m1} and T_{t1} become equal to the corresponding lines of the pure Hopfield model.

Finally, in order to have an idea about the amount of information stored in the network we have to take into account both the value of the capacity and the retrieval overlap. We follow the approach of [20] based upon the Shannon entropy [21]. This leads straightforwardly to the following information content per number of couplings per spin:

$$I(\alpha, m_1) = \alpha[\tfrac{1}{2}(1 + m_1) \ln(1 + m_1) + \tfrac{1}{2}(1 - m_1) \ln(1 - m_1)]. \tag{12}$$

We remark that only m_1 appears in this formula since for $K_1 = K_2$ we recall that $m_1 = m_2$. We have calculated $I(\alpha, m_1)$ for all $\alpha < \alpha_c$ and figure 5 shows its maximal value, I, as a function of K_1^{-1} and K_3^{-1}. A few remarks are in order. First, we find that the maximal information content is reached for values of α slightly smaller than α_c. Second, the greatest information, i.e. $I = 0.1576$, is obtained for equal coupling strengths. Third, for $w = \infty$ we find a constant information content independent of J_3 which is equal to the one in the Hopfield model at zero temperature. This Hopfield value is 0.1213 (see [20]): i.e., 0.0809 in figure 5 in view of the rescaling with $\tfrac{2}{3}$ due to the different number of couplings per spin. Finally, for $w = 0$ and $0 \leqslant K_1^{-1} \leqslant 2$ the critical capacity is equal to the Hopfield value and zero for $K_1^{-1} > 2$ but the information content is continuously going to zero as K_1^{-1} tends to 2. This is due to the fact that the overlap $m_1 = m_2$ corresponding to maximal information goes continuously to zero.

5. Concluding remarks

In this paper we have studied the thermodynamic and retrieval properties of the ATNN neural network model storing an infinite number of patterns using replica-symmetric mean-field theory. This analysis extends our results for this model in the case of low loading [1].

We have derived the free energy and fixed-point equations for the relevant order parameters and have obtained the phase diagram for arbitrary values of the coupling strength of the two- and four-neuron interactions. This model can be considered as the sum of two interacting binary networks such that it contains the Hopfield model when some of the couplings go to zero. For equal coupling strengths this model strongly resembles the four-state Potts neural network.

The storage capacity defined as the number of patterns per number of couplings per spin is maximal for equal coupling strengths and equal to 0.1851. In that case the maximal information content per coupling is 0.1576 versus 0.1213 for the Hopfield model.

Different retrieval characteristics can be distinguished in the phase diagram depending on the parameters of the network. First, the two types of embedded patterns are retrieved and the retrieval quality is enhanced by the interaction between the networks. These retrieval states are the simple Mattis states. Second, the two types of embedded patterns are retrieved but with lower precision because of the presence of this interaction. These retrieval states are the crossed states of the type $mm0$ and mmm. They do not play an important role in the thermodynamics of the model. Third, a pure Hopfield-like phase is present indicating the retrieval of only one kind of pattern.

These results allow us to mention some possible biological applications of this model. Patterns related with two different order parameters may be seen as a representation for two different stimuli: e.g., two visual ones as shape and colour, or two different ones as colour and flavour. When these two stimuli are somehow linked, e.g. through the fact that they were experienced at the same time, it is very likely that they will be recalled together, what corresponds to a suggestion in [4] that particular combinations of stimuli are favoured.

Finally, we remark that there is some re-entrant behaviour in the phase diagram at low temperatures which points at replica-symmetry breaking effects. Calculation of the zero-temperature entropy supports the expectation that this breaking is weak.

In brief, the presence of a four-neuron coupling term in the ATNN model not only enhances the quality of pattern retrieval (by giving a larger overlap at higher temperatures), as present already in the case of low loading [1], but it also increases the critical capacity and the maximal information content in comparision with the Hopfield model.

Acknowledgments

References

[1]   Bollé D and Kozłowski P 1998 *J. Phys. A: Math. Gen.* **31** 6319
[2]   Hopfield J J 1982 *Proc. Natl Acad. Sci. USA* **79** 2554
[3]   Amit D J, Gutfreund H and Sompolinsky H 1987 *Ann. Phys., NY* **173** 30
[4]   Komatsu H and Ideura Y 1993 *J. Neurophysiol.* **70** 677
[5]   Squire L R 1993 *Brain Mechanisms of Perception and Memory* ed T Ono *et al* (Oxford: Oxford University Press) p 219
      Squire L R 1986 *Science* **232** 1612
[6]   Caticha N 1994 *J. Phys. A: Math. Gen.* **27** 5501
[7]   Fontanari J F and Köberle F 1988 *J. Phys. France* **49** 13
[8]   van Hemmen J L 1986 *Phys. Rev.* A **34** 3435
[9]   Kanter I 1988 *Phys. Rev.* A **37** 2739
[10] Bollé D, Dupont P and Huyghebaert J 1992 *Phys. Rev.* A **45** 4194
[11] Huyghebaert J 1994 *PhD Thesis* K U Leuven, Belgium
[12] Kamieniarz G, Kozłowski P and Dekeyser R 1997 *Phys. Rev.* E **55** 3724
[13] Nobre F D and Sherrington D 1993 *J. Phys. A: Math. Gen.* **26** 4539
[14] Cook J 1989 *J. Phys. A: Math. Gen.* **22** 2057
[15] Steffan H and Kühn R 1994 *Z. Phys.* B **95** 249
[16] Bollé D and Huyghebaert J 1995 *Phys. Rev.* E **51** 732
[17] Gerl F and Krey U 1994 *J. Phys. A: Math. Gen.* **27** 7353
[18] Naef J-P and Canning A 1992 *J. Physique* I **2** 247

[19] Canning A and Naef J-P 1992 *J. Physique* I **2** 1791
[20] Amit D J, Gutfreund H and Sompolinsky H 1987 *Phys. Rev.* A **35** 2293
[21] Shannon C E 1948 *Bell Syst. Tech. J.* **27** 379